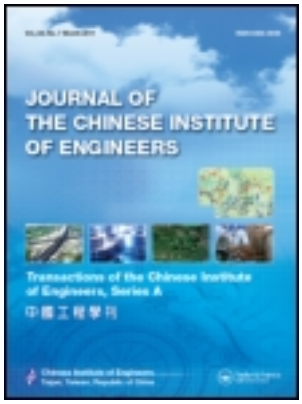

Journal of the Chinese Institute of Engineers
Publication details, including instructions for authors and subscription information:
http://www.tandfonline.com/loi/tcie20

Numerical study of variations of airflow induced by a moving automatic guided vehicle in a cleanroom

Suh-Jenq Yang [a] , Shih-Fa Chen [b] & Wu-Shung Fu [b]

[a] Department of Industrial Engineering and Management , Nan Kai College , Nantou, Taiwan 542, R.O.C.

[b] Department of Mechanical Engineering , National Chiao Tung University , Hsinchu, Taiwan 300, R.O.C.

Published online: 03 Mar 2011.

To cite this article: Suh-Jenq Yang , Shih-Fa Chen & Wu-Shung Fu (2002) Numerical study of variations of airflow induced by a moving automatic guided vehicle in a cleanroom, Journal of the Chinese Institute of Engineers, 25:1, 67-75, DOI: 10.1080/02533839.2002.9670681

To link to this article: http://dx.doi.org/10.1080/02533839.2002.9670681

NUMERICAL STUDY OF VARIATIONS OF AIRFLOW INDUCED BY A MOVING AUTOMATIC GUIDED VEHICLE IN A CLEANROOM

Suh-Jenq Yang
Department of Industrial Engineering and Management
Nan Kai College
Nantou, Taiwan 542, R.O.C.

Shih-Fa Chen and Wu-Shung Fu*
Department of Mechanical Engineering
National Chiao Tung University
Hsinchu, Taiwan 300, R.O.C.

Key Words: cleanroom, AGV, recirculation zones, FEM.

ABSTRACT

The variations of airflow induced by a moving automatic guided vehicle (AGV) in a vertical laminar flow cleanroom are studied numerically. From a viewpoint of fluid mechanics, the characteristic of the variations of the airflow induced by a moving object is dynamic and is classified as a moving boundary problem. A Galerkin finite element formulation with an arbitrary Lagrangian-Eulerian (ALE) kinematic description method is adopted to analyze this problem. Three different moving velocities of the AGV under Reynolds number *Re*=500 and two different positions of the wafer cassette are considered. The results show that the formation of recirculation zones, which are disadvantageous for removing contaminants, is remarkably dependent on the moving velocity of the AGV and the position of the wafer cassette.

I. INTRODUCTION

Recently, accompanying state-of-the-art semiconductor techniques, wafers have increased in both size and weight. It has become difficult for an operator without any auxiliary tools to carry the larger and heavier wafers. Thus, an effective transport tool is required to save labor and decrease wafer damage and contamination. An AGV is commonly used in a cleanroom for transporting wafers.

In the past, most studies about AGVs were focused on the characteristics, system control, and path planning. Among studies devoted to the characteristics of the AGV, McClelland (1986) described the potential advantages of the utilization of the AGV in the semiconductor industry to prevent contamination. Lee *et al*. (1996) used five heuristic rules to deal with the load selection of the AGV. Rajotia *et al*. (1998) employed analytical and simulation modeling to determine the number of AGVs needed. Referring to the literature of process control, Zaremba *et al*. (1997) adopted max-algebra formalism for the robust distributed control of the AGV. Funabiki and Kodera (1998) proposed a steering control strategy of the AGV with successive learning neural networks using a real-time tuning function. Kim *et al*. (1999) utilized a deadlock prevention algorithm to describe the dispatching problem based on workload balancing for the control of the AGV. Concerning research on path planning, Lin and Wang (1997) proposed a fuzzy

*Correspondence addressee

approach, which included sensor modeling and trap recovering to prevent collision with unknown moving obstacles. Oboth *et al*. (1999) adopted a large-scale simulation of a dynamic batch type to present a route-generation technique that provided conflict-free routes for multiple AGVs. Sekine *et al*. (1999) used the imbedded Markov chain method to deal with the analysis of traffic congestion among AGVs.

As for the other important issue, the effect of the AGV on the motions of the airflow in the cleanroom has been relatively less studied. Kanayama et al. (1993) adopted a numerical method to analyze a two-dimensional flow around an AGV in a cleanroom. The results showed that the wafer might not be contaminated by particles from the floor. However, to facilitate the analysis, the study mentioned above regarded the moving AGV as a stationary one, which resulted in the phenomena of the airflow being rather different from what actually occurs.

Consequently, the aim of this study is to numerically simulate the motions of the airflow affected by a moving AGV in the cleanroom. Because of the movement of the AGV, this subject is classified as a moving boundary problem, which is difficult to analyze solely using either the Lagrangian or Eulerian kinematic description method. An appropriate kinematic description method of the ALE method, which combines the characteristics of the Lagrangian and Eulerian kinematic description methods, is adopted to describe this problem. In the ALE method, the computational meshes may move with the fluid (Lagrangian), be held fixed (Eulerian), or be moved in any other prescribed way. The details of the kinematic theory of the ALE method are given in Hughes *et al*.. (1981), Donea *et al*. (1982), and Ramaswamy (1990). A Galerkin finite element method with moving meshes and an implicit difference scheme, dealing with the time terms, is used to solve the governing equations. Three different moving velocities of the AGV and two different positions of the wafer cassette are considered. The results show that the formation of recirculation zones around the AGV and wafer cassette is remarkably dependent on the moving velocity of the AGV and the position of the wafer cassette. These phenomena are quite different from those shown in Kanayama *et al*. (1993) in which the moving AGV was regarded as a stationary one.

II. PHYSICAL MODEL

A model of a two-dimensional vertical laminar flow cleanroom sketched in Fig. 1 is used. The height and width of the cleanroom are $h(=h_1+h_2+h_3)$ and w, respectively. Two workbenches, with height h_2 and width w_1, are set on the right and left sides of the cleanroom, respectively. An AGV, with height h_5 and

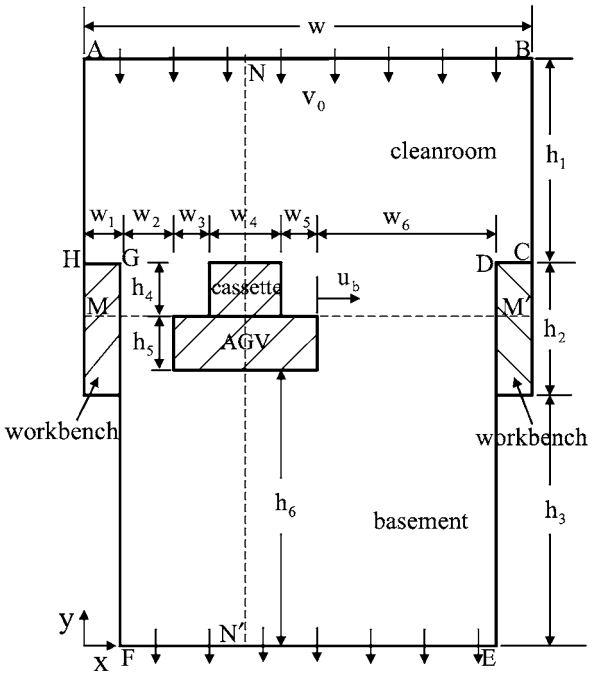

Fig. 1 Physical model.

width $w_8(=w_3+w_4+w_5)$, moves between the two workbenches. The wafer cassette, with height h_4 and width w_4, is put on the top surface of the AGV. The inlet air, velocity v_0, flows into the cleanroom at the inlet section AB. Initially (t=0), the distance from the left workbench to the AGV is w_2, and the AGV is stationary and the airflow flows steadily. As the time t>0, the AGV moves toward the right workbench with a constant velocity u_b. The interaction between the airflow and AGV affects the behavior of the airflow in the cleanroom. This subject is classified as a moving boundary problem and becomes a time-dependent problem. Thus, the ALE method is properly utilized to analyze this problem.

In order to facilitate the analysis, the following assumptions are made.

(1) The flow field is two-dimensional, incompressible and laminar.
(2) The properties of the fluid are constant and the effect of gravity is neglected.
(3) The no-slip condition is held on the interfaces between the airflow and AGV.

According to the characteristic scales of w_1, v_0 and ρv_0^2, the dimensionless variables are defined as follows:

$$X=\frac{x}{w_1},\quad Y=\frac{y}{w_1},\quad U=\frac{u}{v_0},$$

$$V=\frac{v}{v_0},\quad \hat{U}=\frac{\hat{u}}{v_0},\quad U_b=\frac{u_b}{v_0},$$

$$\mathrm{Re}=\frac{v_0 w_1}{\nu},\quad \tau=\frac{t v_0}{w_1},\quad P=\frac{p-p_\infty}{\rho v_0^2}, \qquad (1)$$

where $\hat{u}$ is the mesh velocity in the x-direction.

Based upon the above assumptions and dimensionless variables, the dimensionless ALE governing equations are expressed as the following equations: continuity equation

$$\frac{\partial U}{\partial X}+\frac{\partial V}{\partial Y}=0 \tag{2}$$

momentum equations

$$\frac{\partial U}{\partial \tau}+(U-\hat{U})\frac{\partial U}{\partial X}+V\frac{\partial U}{\partial Y}=-\frac{\partial P}{\partial X}+\frac{1}{\mathrm{Re}}\left(\frac{\partial^2 U}{\partial X^2}+\frac{\partial^2 U}{\partial Y^2}\right) \tag{3}$$

$$\frac{\partial V}{\partial \tau}+(U-\hat{U})\frac{\partial V}{\partial X}+V\frac{\partial V}{\partial Y}=-\frac{\partial P}{\partial Y}+\frac{1}{\mathrm{Re}}\left(\frac{\partial^2 V}{\partial X^2}+\frac{\partial^2 V}{\partial Y^2}\right) \tag{4}$$

As the time $\tau>0$, the boundary conditions are as follows:

on the wall surfaces of the cleanroom

$$U=V=0, \tag{5}$$

on the airflow inlet section AB

$$U=0,\ V=-1.0, \tag{6}$$

on the airflow outlet section EF

$$\frac{\partial U}{\partial Y}=\frac{\partial V}{\partial Y}=0, \tag{7}$$

on the interfaces of the AGV and the airflow

$$U=U_b,\ V=0. \tag{8}$$

III. NUMERICAL METHOD

A Galerkin finite element formulation with moving meshes and an implicit scheme, dealing with the time terms, is adopted to solve the governing Eqs. (2)-(4). The Newton-Raphson method is used to linearize the nonlinear terms in the momentum equations, and the pressure is eliminated from the momentum equations using the penalty function model (Reddy and Gartling, 1994). Nine node quadrilateral elements are utilized to discretize the problem domain and the velocity terms are approximated using the quadratic shape functions. The discretization processes of the governing equations are similar to the one used in Fu *et al.* (1990). Then, the momentum Eqs. (3)-(4), can be expressed as follows:

$$\sum_{1}^{n_e}([A]^{(e)}+[K]^{(e)}+\lambda[L]^{(e)})\{q\}^{(e)}_{\tau+\Delta\tau}=\sum_{1}^{n_e}\{f\}^{(e)}, \tag{9}$$

where

$$(\{q\}^{(e)}_{\tau+\Delta\tau})^T=\left\langle U_1, U_2, \cdots, U_9, V_1, V_2, \cdots, V_9\right\rangle^{m+1}_{\tau+\Delta\tau}, \tag{10}$$

$[A]^{(e)}$ consists of the (m)th iteration values of U and V at the time $\tau+\Delta\tau$,

$[K]^{(e)}$ consists of the $\hat{U}$ and time differential terms,

$[L]^{(e)}$ consists of the penalty function terms,

$\{f\}^{(e)}$ consists of the known values of U and V at the time τ and (m)th iteration values of U and V at the time $\tau+\Delta\tau$.

In Eq. (9), the terms with the penalty parameter λ are integrated by 2×2 Gaussian quadrature, and the other terms are integrated by 3×3 Gaussian quadrature. The value of penalty parameter used in this study is 10^6, and the frontal method solver Taylor and Hughes (1981) is used to solve Eq. (9).

The mesh velocity $\hat{U}$ is assumed to be linearly distributed and inversely proportional to the distance between the computational meshes and the AGV. To prevent the computational nodes in the vicinity of the AGV slipping away from the boundary layer, the mesh velocities adjacent to the AGV are expediently assigned equal to the velocity of the AGV.

A brief outline of the solution procedure follows:

(1) Determine the optimal mesh distribution and number of elements and nodes.

(2) Solve the values of U and V at the steady state and regard them as the initial values.

(3) Determine the time increment $\Delta\tau$ and the mesh velocities $\hat{U}$ at every node.

(4) Update the coordinates of the nodes and examine the determinant of the Jacobian transformation matrix to ensure the one-to-one mapping is satisfied during the Gaussian quadrature numerical integration; otherwise, execute the mesh reconstruction.

(5) Solve Eq. (9) until the following criteria for convergence are satisfied:

$$\left|\frac{\phi^{m+1}-\phi^{m}}{\phi^{m+1}}\right|_{\tau+\Delta\tau}<10^{-3},\ \text{where } \phi=U, V \tag{11}$$

(6) Continue the next time step calculation until the assigned position of the AGV is reached.

IV. RESULTS AND DISCUSSION

Four cases with different moving velocities and the dimensionless geometric parameters are tabulated in Table 1. Cases 1, 2, and 3, which correspond to the moving velocities U_b=0.5, 2.0, and 4.0,

Table 1 The dimensionless geometric parameters of the cleanroom for four different cases

	U_b	H_1	H_2	H_3	H_4	H_5	H_6	W	W_1	W_2	W_3	W_4	W_5	W_6
case 1	0.5	7	4	34	1	1	36	22	1	4	1	2	1	12
case 2	2.0	7	4	34	1	1	36	22	1	4	1	2	1	12
case 3	4.0	7	4	34	1	1	36	22	1	4	1	2	1	12
case 4	2.0	7	4	34	1	1	36	22	1	4	0.25	2	1.75	12

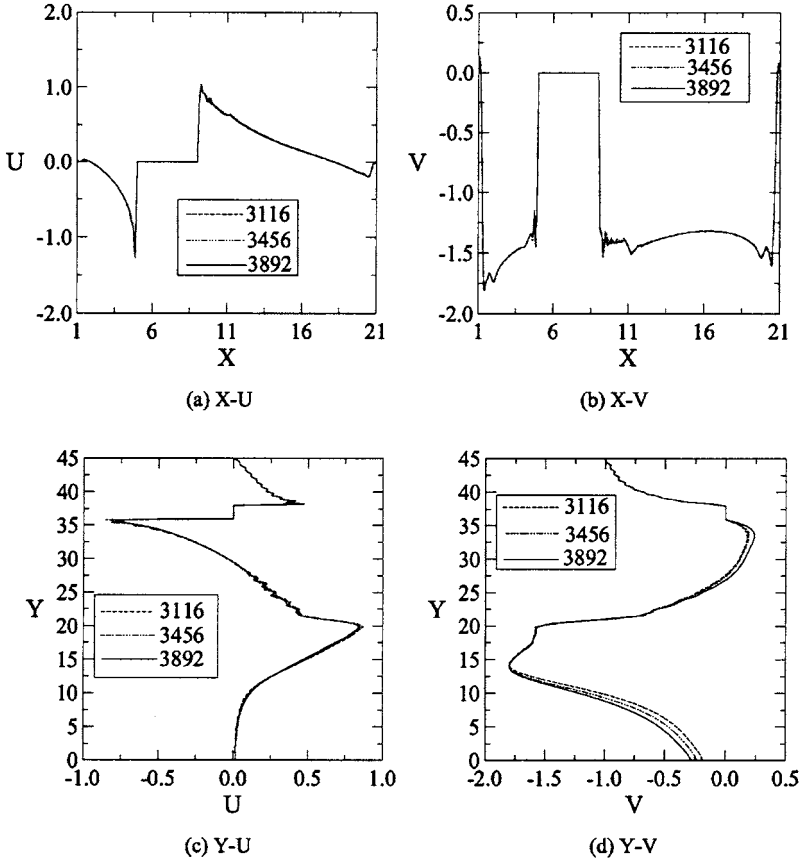

Fig. 2 Comparison of the distributions of the velocities U and V along the lines of MM' and NN' at the steady state and Re=500 for various meshes (a) X-U, (b) X-V, (c) Y-U, (d) Y-V

respectively, have the same geometric condition. Case 4 has the same moving velocity as case 2, but the position of the wafer cassette in case 4 is on the left top surface of the AGV. The variations of the airflow induced by the movement of the AGV under Re=500 are examined in detail.

For matching the boundary conditions at the inlet and outlet of the cleanroom mentioned earlier, the lengths from the inlet and outlet to the AGV are determined by numerical tests and are equal to 8.0 and 36.0, respectively. To obtain an optimal computational mesh, three different nonuniform distributed elements 3116, 3456, and 3892 (corresponding to 12572, 14124, and 15892 nodes, respectively) are tested for case 1 as the AGV is stationary. The results of the distributions of velocities U and V along the lines MM' and NN', as indicated in Fig. 1, are shown in Fig. 2. According to the results of the mesh tests, the computational mesh with 3892 elements is adopted for cases 1, 2, and 3. Similarly, the nonuniform distribution of 4000 elements corresponding to 16332 nodes is adopted for case 4. Moreover, an implicit scheme is employed to deal with the time differential terms of the governing equations. The time step $\Delta\tau$=0.005 is chosen for all cases in this study.

To illustrate the variations of the airflow in more detail, we only presented the velocity vectors around the AGV and wafer cassette. Besides, the

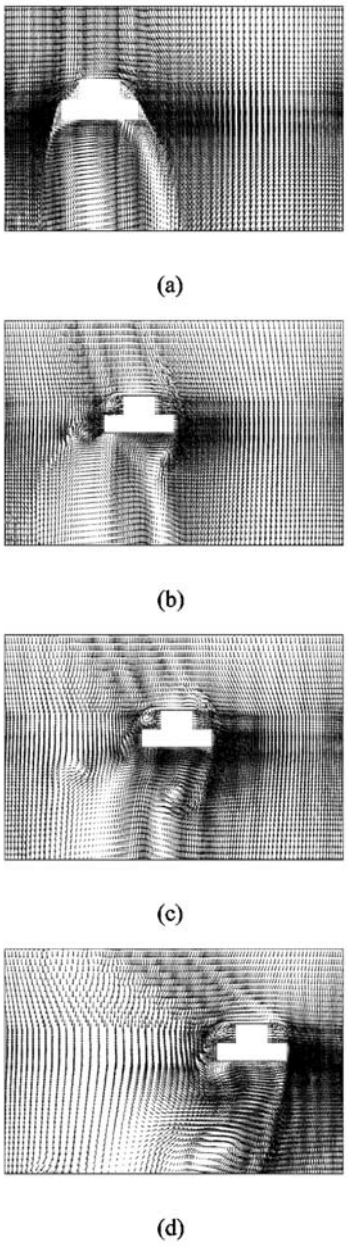

Fig. 3 The transient developments of the velocity vectors around the AGV and wafer cassette for case 1 (U_b=0.5) (a) τ=0.0, (b) τ=4.0, (c) τ=8.0, (d) τ=16.0

velocity vectors shown in the following figures are scaled relative to the maximum velocity in the flow field.

Figure 3 shows the transient developments of the velocity vectors around the AGV and wafer cassette for case 1. In this case, the moving velocity U_b of the AGV is 0.5. At the time τ=0.0, as shown in Fig. 3(a), the AGV is stationary and the distance w_2 is equal to 4.0. The airflow flows downward, steadily. A large recirculation zone is observed near the bottom surface of the AGV. As the time τ>0.0, the AGV moves toward the right workbench with a constant moving velocity U_b=0.5. Thus, the variations of the flow field become the transient state. Because the velocity of the inlet airflow is larger than the moving velocity of the AGV, the AGV seems to be an obstacle in the way of the airflow. At the time τ=4.0 (Fig. 3(b)), the AGV presses the airflow near the front surface of the AGV, and the direction of the airflow is forced to change and turn into the bottom surface of the AGV. As for the airflow near the rear region of the AGV, the inlet airflow simultaneously replenishes the vacant space induced by the movement of the AGV. Consequently, new recirculation zones are formed around the rear region of the AGV and cassette. Particles might suspend in these recirculation zones near the AGV and cassette and are difficult for the airflow to remove. As the time increases, as shown in Figs. 3(c)-(d), the recirculation zones around the rear region of the AGV and cassette enlarge gradually, and the variations of the airflow around the AGV become more complex. These phenomena are disadvantageous to removal of particles from the cleanroom. Furthermore, because of the moving of the AGV, some of the airflow flowing through the rear region of the AGV flows toward the bottom surface of the AGV. As a result, the airflow might sweep particles from the floor to the work areas and this is disadvantageous for the semiconductor manufacturing process. The results are remarkably different from those shown in Kanayama *et al.* (1993), which regarded the moving AGV as a stationary one.

Figure 4 shows the transient developments of the velocity vectors around the AGV and wafer cassette for case 2. In this case, the AGV moves toward the right workbench with a constant velocity U_b= 2.0, which is much faster than that of the above case. In the first stage of the transient state, as shown in Fig. 4(b), the variations of the airflow are similar to the above case. As the time increases, as shown in Figs. 4(c)-(d), because the moving velocity of the AGV is faster than that of case 1, the recirculation zones around the AGV and cassette are larger in this case.

The transient developments of the velocity vectors around the AGV and wafer cassette for case 3, in which the moving velocity of the AGV is equal to 4.0, are shown in Fig. 5. Basically, the variations of the flow field are similar to case 2. However, the strengths of recirculation zones around the rear region of the AGV and cassette are stronger than those of the above cases; that is disadvantageous for re-moving particles. Besides, because of the friction between the AGV and rail, the increase of the moving velocity of the AGV will produce more particles, which results in serious contamination on the products.

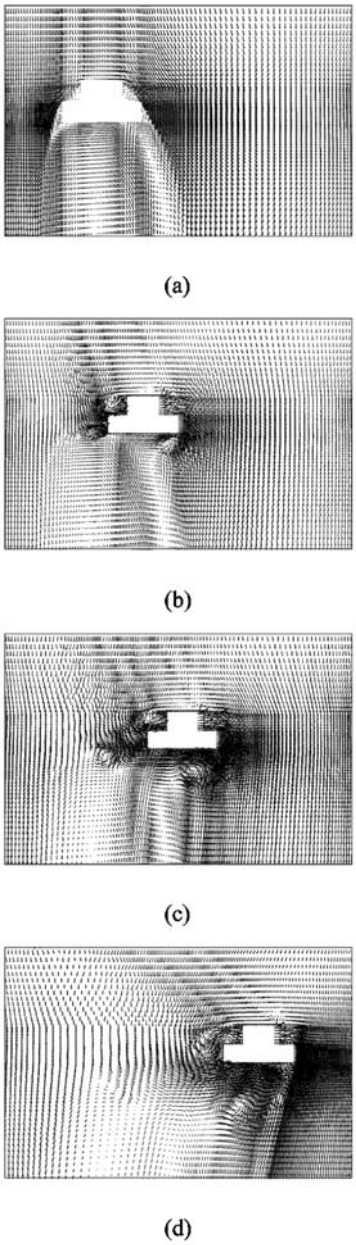

Fig. 4 The transient developments of the velocity vectors around the AGV and wafer cassette for case 2 (U_b=2.0) (a) τ=0.0, (b) τ=1.0, (c) τ=2.0, (d) τ=4.0

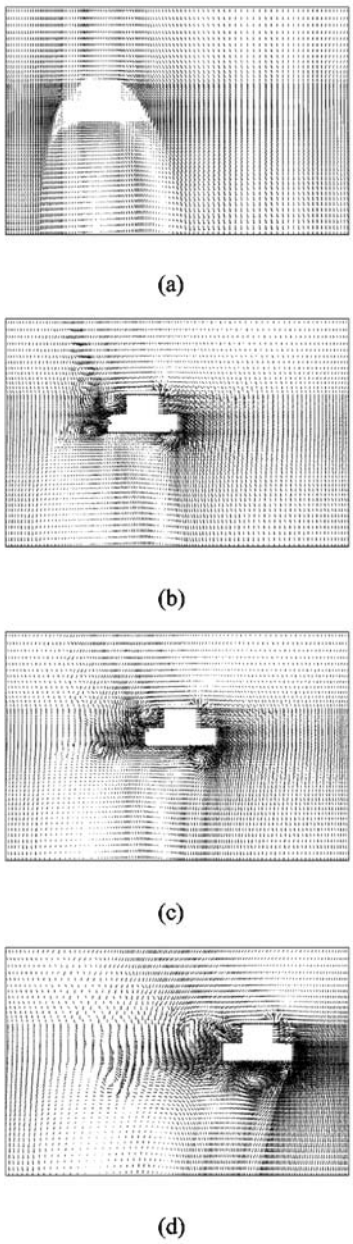

Fig. 5 The transient developments of the velocity vectors around the AGV and wafer cassette for case 3 (U_b=4.0) (a) τ=0.0, (b) τ=0.5, (c) τ=1.0, (d) τ=2.0

As shown in Fig. 6, there are the transient developments of the velocity vectors around the AGV and wafer cassette for case 4, in which the moving velocity of the AGV is the same as case 2, but the wafer cassette is near the left side of the top surface of the AGV. At the time τ=1.0, the recirculation zones around the rear region of the AGV and cassette are similar to case 2; however, the recirculation zone near the cassette is larger than that of case 2. At the time τ=2.0, the recirculation zones around the rear region of the AGV and cassette enlarge gradually. As the time increases, the recirculation zones around the rear region of the AGV and cassette shrink gradually; these phenomena are somewhat different from those in case 2. Therefore, the position of the wafer cassette near the lateral side seems to be better than that in the central region of the top surface of the AGV.

V. CONCLUSIONS

The variations of the airflow induced by the movement of an AGV in a cleanroom are investigated numerically. The main conclusions can be summarized as follows:

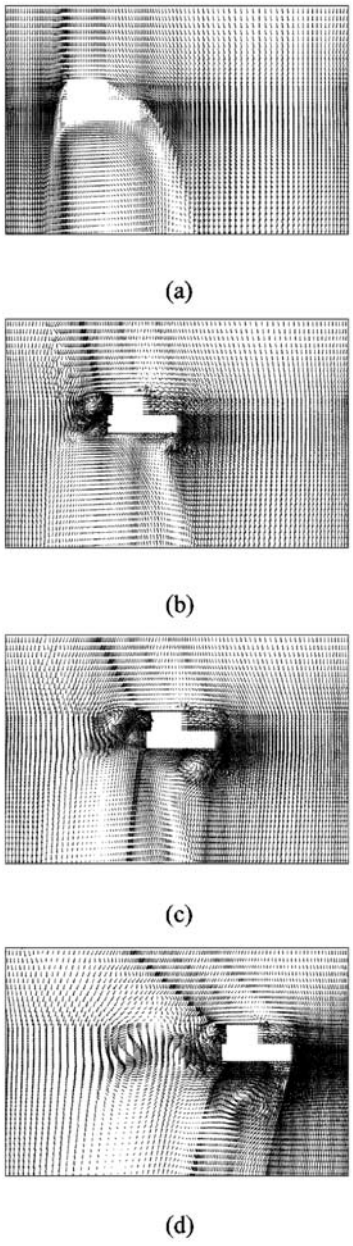

Fig. 6 The transient developments of the velocity vectors around the AGV and wafer cassette for case 4 (U_b=2.0) (a) τ=0.0, (b) τ=1.0, (c) τ=2.0, (d) τ=4.0

1. The recirculation zones, in which particles are easily trapped, are observed around the AGV and wafer cassette as the AGV moves. The results are different from studies regarding a moving AGV as a stationary one.
2. The lower the moving velocity of the AGV, the smaller the recirculation zones formed.
3. From a viewpoint of contamination control, the position of the wafer cassette near either side of the top surface of the AGV is better than that in the central region of the top surface of the AGV.

ACKNOWLEDGEMENT

The support of this work by the National Science Council of Taiwan, R.O.C., under contract NSC90-2626-E-252-003 is gratefully acknowledged.

NOMENCLATURE

h	the height of the cleanroom [m]
H	dimensionless height of the cleanroom
h_1	the distance from the workbench to the ceiling of the cleanroom [m]
H_1	dimensionless distance from the workbench to the ceiling of the cleanroom
h_2	the height of the workbench [m]
H_2	dimensionless height of the workbench
h_3	the distance from the workbench to the outlet [m]
H_3	dimensionless distance from the workbench to the outlet
h_4	the height of the cassette [m]
H_4	dimensionless height of the cassette
h_5	the height of the AGV [m]
H_5	dimensionless height of the AGV
h_6	the distance from the AGV to the outlet [m]
H_6	dimensionless distance from the AGV to the outlet
p	pressure [N/m^2]
p_∞	reference pressure [N/m^2]
P	dimensionless pressure
Re	Reynolds number
t	time [s]
u, v	velocities of the airflow in x and y directions [m/s]
U,V	dimensionless velocities of the airflow in X and Y directions
u_b	the moving velocity of the AGV [m/s]
U_b	dimensionless moving velocity of the AGV
$\hat{u}$	the mesh velocity in x-direction [m/s]
$\hat{U}$	dimensionless mesh velocity in X-direction
v_0	the airflow inlet velocity [m/s]
V_0	dimensionless airflow inlet velocity
w	the width of the cleanroom [m]
W	dimensionless width of the cleanroom
w_1	the width the of workbench [m]
W_1	dimensionless width of the workbench
w_2	the distance from the left workbench to the AGV [m]
W_2	dimensionless distance from the left workbench to the AGV
w_4	the width of the cassette [m]
W_4	dimensionless width of the cassette
w_6	the distance from the AGV to the right workbench [m]
W_6	dimensionless distance from the AGV to the right workbench

x, y Cartesian coordinates [m]
X, Y dimensionless Cartesian coordinates

Greek

λ penalty parameter
ν kinematic viscosity [m^2/s]
ρ density [kg/m^3]
τ dimensionless time

Other

[] matrix
{} column vector
<> row vector
| | absolute value

REFERENCES

1. Donea, J., Giuliani, S., and Halleux, J. P., 1982, "An Arbitrary Lagrangian-Eulerian Finite Element Method for Transient Dynamic Fluid-structure Interactions," *Computer Methods in Applied Mechanics and Engineering*, Vol. 33, pp. 689-723.
2. Fu, W. S., Kau, T. M., and Shieh, W. J., 1990, "Transient Laminar Natural Convection in an Enclosure from Steady Flow State to Stationary State," *Numerical Heat Transfer*, Part A, Vol. 18, pp. 189-211.
3. Funabiki, S. and Kodera, K., 1998, "A Steering Control of Automated Guided Vehicles by the Neural Networks Using a Real-time Function," *Transactions of the Institute of Electrical Engineers Japan*, Part D, Vol. 118, No. 5, pp. 605-610.
4. Hughes, T. J. R., Liu, W. K., and Zimmermann, T. K., 1981, "Lagrangian-Eulerian Finite Element Formulation for Incompressible Viscous Flows," *Computer Methods in Applied Mechanics and Engineering*, Vol. 29, pp. 329-349.
5. Kanayama, H., Toshigami, K., Tashiro, Y., Tabata, M., and Fujima, S., 1993, "Finite Element Analysis of Air Flow Around an Automatic Guided Vehicle," *Journal of Wind Engineering and Industrial Aerodynamics*, Vol. 46-47, pp. 801-810.
6. Kim, C. W., Tanchoco, J. M. A., and Koo, P. H., 1999, "AGV Dispatching Based on Workload Balancing," *International Journal of Production Research*, Vol. 37, No. 17, pp. 4053-4066.
7. Lee, J., Tangjarukij, M., and Zhu, Z., 1996, "Load Selection of Automated Guided Vehicles in Flexible Manufacturing Systems," *International Journal of Production Research*, Vol. 34, No. 12, pp. 3383-3400.
8. Lin, C. H. and Wang L. L., 1997, "Intelligent Collision Avoidance by Fuzzy Logic Control," *Robotics and Autonomous Systems*, Vol. 20, No. 1, pp. 61-83.
9. McClelland, S., 1986, "The Cleanest Robots in the World' (Clean Room Robots)," *The Industrial Robot*, Vol. 13, No. 4, pp. 217-220.
10. Oboth, C., Batta, R., and Karwan M., 1999, "Dynamic Conflict-Free Routing of Automated Guided Vehicles," *International Journal of Production Research*, Vol. 37, No. 9, pp. 2003-2030.
11. Rajotia, S., Shanker, K., and Batra, J. L., 1998, "Determination of Optimal AGV Fleet Size for an FMS," *International Journal of Production Research*, Vol. 36, No. 5, pp. 1177-1198.
12. Ramaswamy, B., 1990, "Numerical Simulation of Unsteady Viscous Free Surface Flow," *Journal of Computational Physics*, Vol. 90, pp. 396-430.
13. Reddy, J. N. and Gartling, D. K., 1994, The Finite Element Method in Heat Transfer and Fluid Dynamics, CRC Press. Inc., Ann. Arbor, chapter 4.
14. Sekine, E., Hamamatsu, Y., and Kongouji, T., 1999, "Analysis of Traffic Congestion in AGV System," *Transactions of the Institute of Electrical Engineers Japan*, Part D, Vol. 119, No. 4, pp. 515-522.
15. Taylor, C. and Hughes, T. G., 1981, *Finite Element Programming of the Navier-Stokes Equations*, Pineridge Press Ltd., U.K., chapter 6.
16. Zaremba, M. B., Obuchowicz, A., Banaszak, Z. A., and Jedrzejek, K. J., 1997, "A Max-Algebra Approach to the Robust Distributed Control of Repetitive AGV Systems," *International Journal of Production Research*, Vol. 35, No. 10, pp. 2667-2687.

Manuscript Received: Apr. 09, 2001
Revision Received: Aug. 07, 2001
and Accepted: Oct. 02, 2001

以數值方法探討潔淨室中無人自動化車移動所誘導的流場變化

楊肅正

南開技術學院工業工程與管理科

陳石法　傅武雄

國立交通大學機械工程學系

摘　要

本研究以數值方法探討潔淨室中無人自動化車移動所誘導的流場變化，這種物理現象在流體力學上是屬於動態的移動邊界問題。本研究採用『任意拉格朗日—尤拉』座標系統描述流場的運動，並以具處罰函數模式之葛拉金有限元素法模擬流場的變化。在雷諾數 Re=500 條件下，針對三種不同的無人自動化車移動速度和兩種不同的晶圓匣置放位置，探討流場受無人自動化車移動所誘導的流場變化。結果顯示，無人自動化車移動速率之快慢和晶圓匣置放位置是決定回流區形式的主要因素，而回流區將不利於污染物的排除，影響產品的可靠度與品質。

關鍵詞：潔淨室，無人自動化車，回流區，有限元素法。